

An integrated microfluidic chip with 40 MHz lead-free transducer for fluid analysis

S. T. F. Lee,^{a)} K. H. Lam, L. Lei, X. M. Zhang, and H. L. W. Chan

Department of Applied Physics and Materials Research Centre, The Hong Kong Polytechnic University, Kowloon, Hong Kong

(Received 28 December 2010; accepted 19 January 2011; published online 25 February 2011)

The design, fabrication, and evaluation of a high-frequency transducer made from lead-free piezoceramic for the application of microfluidic analysis is described. Barium strontium zirconate titanate [(Ba_{0.95}Sr_{0.05})(Zr_{0.05}Ti_{0.95})O₃, abbreviated as BSZT] ceramic has been chosen to be the active element of the transducer. The center frequency and bandwidth of this high-frequency ultrasound transducer have been measured to be 43 MHz and 56.1%, respectively. The transducer was integrated into a microfluidic channel and used to measure the sound velocity and attenuation of the liquid flowing in the channel. Results suggest that lead-free high-frequency transducers could be used for *in situ* analysis of property of the fluid flowing through the microfluidic system. © 2011 American Institute of Physics. [doi:10.1063/1.3553575]

I. INTRODUCTION

Microfluidics have been widely used in the fields of biology and chemistry due to various advantages which include the ability to use very small amount of samples, low cost, short time for analysis, high detection resolution, and sensitivity, etc.^{1–3} The rapid development of microfabrication technology has allowed us to miniaturize biological and chemical processes, which brings about the field of micro-total-analysis system (μ -TAS), also called “lab-on-a-chip” which includes separation, treatment, and detection of various samples.^{4,5} For liquids (e.g., oil and petrol), the acoustic velocity, density, concentration, and attenuation are important physical properties that help to characterize their quality. Conventionally, optical and electrochemical methods are used in microfluidic analyses. Recently, a pair of piezoelectric lead magnesium niobate-lead titanate (PMN-PT) single crystal transducers was used to measure the velocity and attenuation of the liquid flowing in a microfluidic system.⁶ Here, we present a similar acoustic detection method using one lead-free high-frequency transducer.

Lead-based piezoelectric materials, such as PMN-PT and lead zirconate titanate (PZT), are often used as the active element to fabricate transducers due to their high piezoelectric coefficient and high thickness mode electromechanical coupling coefficient.^{7,8} However, lead-based materials contain lead which is toxic and is a hazard to the environment. Many countries have banned the use of lead-based materials (e.g., in lead soldering) and, therefore, it is important to replace the lead-based materials with lead-free materials for environmental protection.^{9,10} (Ba_{0.95}Sr_{0.05})(Zr_{0.05}Ti_{0.95})O₃ (BSZT) ceramics have been reported to have good piezoelectric properties and have been used in making device such as stepped horn transducer.^{10,11} In this work, the fabrication of a high-frequency lead-free BSZT transducer is described and its performance evaluated by means of a pulse-echo method.

A BSZT transducer with a center frequency of \sim 43 MHz has been integrated into a microfluidic system prepared by a soft-photolithographic method using polydimethylsiloxane (PDMS). The microfluidic device is then used to evaluate various important physical properties of the liquid medium flowing within the channel.

II. EXPERIMENTAL

A. Fabrication of the BSZT needle transducer

A conventional mixed oxide technique was used to prepare the BSZT ceramic discs of 1.3 mm diameter¹⁰ using reagent grade metal oxides and carbonate powders. A conductive backing material E-Solder 3022 (VonRoll Isola, New Haven, CT) was cured on one side of the BSZT ceramic disc. The other side of the disc was lapped to the designated thickness of 60 μ m. With the use of a dicing saw (Model DAD 321, DISCO, Japan), the active element with dimensions of 0.9 mm \times 0.9 mm was cut out. A copper wire was adhered to the conductive backing and the element was fixed into a stainless steel housing (Fig. 1) by epoxy (Ciba-Geigy, 5 min Araldite). Subsequently, the BSZT element was electrically connected to the stainless steel tube (2.2 mm diameter) housing using a thin layer of silver paint, forming the common ground connection. The transducer was then poled under an electrical field of 3 kV/mm at 25 °C for 30 min to elicit the piezoelectric properties of the BSZT ceramics.

The fabricated BSZT ceramics were measured using a d_{33} meter (ZJ-30 piezo d_{33} meter) and found to have a large piezoelectric coefficient of 300 pC/N. A thickness mode electromechanical coupling factor of 0.45 was found using the resonance technique. A clamped dielectric constant ϵ_{33}^s of 1346 and a loss tangent $\tan \delta = 2.5\%$ were measured at 5 MHz. In order to match 50 Ω impedance of the driving circuit, the transducer has to be fabricated into an area of 0.9 mm \times 0.9 mm. The area is determined by the equation

$$A = \frac{Ct}{\epsilon_{33}^s \epsilon_0}, \quad (1)$$

^{a)}Corresponding author: Tel: +852-27664162; Fax: +852-23337629. E-mail address: felix_leo6288@hotmail.com.

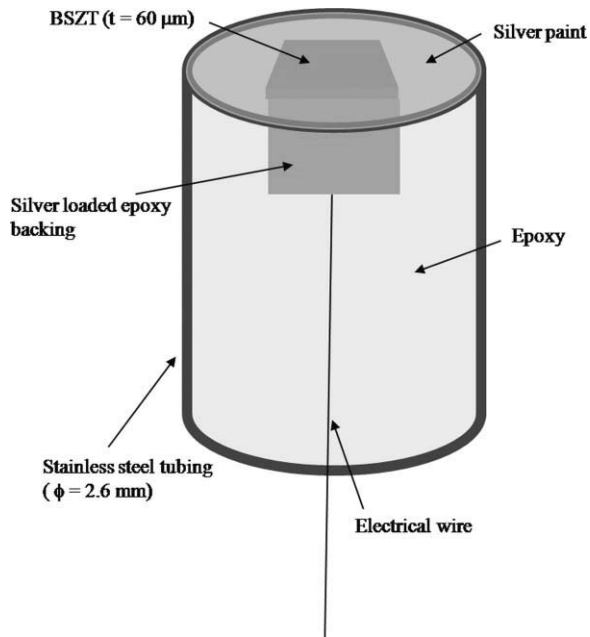


FIG. 1. (Color online) Schematic diagram of the BSZT transducer.

where C is the capacitance at 5 MHz, t is the thickness, ϵ_{33}^S is the clamped dielectric constant, and ϵ_0 is the permittivity of vacuum. The capacitance can be estimated using the equation

$$C = \frac{1}{2\pi f Z}, \quad (2)$$

where f is the resonance frequency (~ 43 MHz) and Z is the electrical impedance which is 50Ω .

To determine the center frequency, bandwidth, and insertion loss of the transducer, a pulse-echo response arrangement was employed. The transducer, mounted in a water tank in front of a thick stainless steel target, was connected to a Panametrics 5900PR pulser/receiver. The testing distance was at a^2/λ in the far field region, where a is the radius of the transducer and λ is the acoustic wavelength in water at the resonance frequency. The transducer was excited by $1 \mu\text{J}$ electrical impulse with 1 kHz repetition rate and 50Ω damping. The echo response was displayed on an oscilloscope (HP Infinium) captured by the circuit of the 5900PR together with the frequency spectrum calculated by the built-in fast-Fourier-transform math feature on the oscilloscope. The two-way insertion loss was measured by a Tektronix AFG 3251 function generator with 50Ω output impedance. A tone burst of a 20-cycle sine wave with an amplitude of 1 V was generated at the center frequency of the transducer, as measured by the oscilloscope with 50Ω coupling. By connecting the transducer to the function generator, the voltage amplitude of received echo was measured by the oscilloscope with $1 \text{ M}\Omega$ coupling.

B. Fabrication of the microfluidic system

The microfluidic channel was made up of two parts. The bottom part was formed by a PDMS mixture with a ratio of 10:1 prepolymer and crosslinking polymer. It was cured at 85°C for 1 hr and is 3 mm thick. The transducer was fixed into a tube of slightly larger diameter (2.6 mm) to enable a smooth movement along its axial direction, and a nonhardening

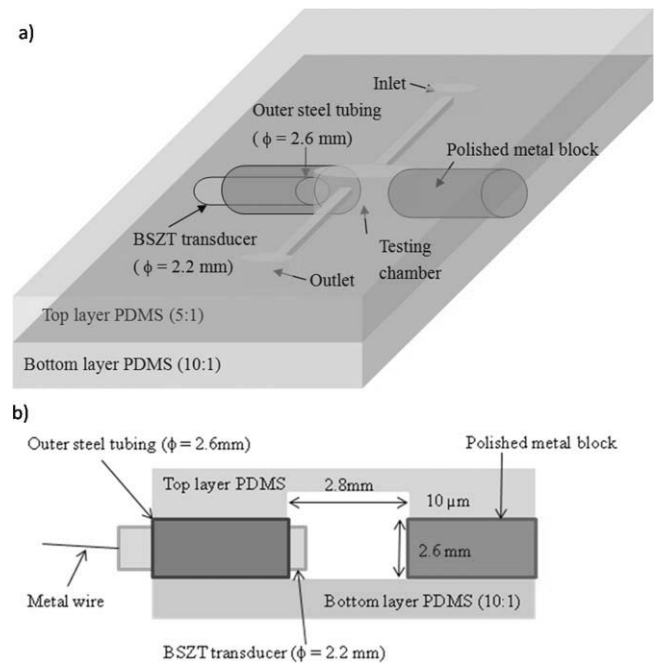


FIG. 2. (Color online) Design of the microfluidic system. (a) Top-view of the microfluidic system. (b) Cross-sectional view of the microfluidic system.

gasket joining compound (Loctite Ultra Black) was added to prevent leakage of the liquid during measurement. The transducer was then fixed into the bottom layer of PDMS. A polished metal block (2.6 mm diameter) was fixed at 2.8 mm away from the transducer to reflect the ultrasonic pulse. A chamber was formed by cutting away the PDMS ($2.6 \text{ mm} \times 2.8 \text{ mm} \times 2.6 \text{ mm}$) between the transducer and the metal block and by the cylindrical cavity of radius 1.4 mm in the upper PDMS block. The schematic diagram of the microfluidic system is shown in Fig. 2. To fabricate the Si mold for the upper part of the channel, a thin layer of photoresist was spun on a silicon wafer and patterned by a high precision plastic mask. Lithographic techniques were employed to develop the channel pattern. PDMS of ratio 5:1 was poured onto the Si mold. After curing, the PDMS was peeled off from the mold. The channel has a height of $10 \mu\text{m}$. Finally, oxygen plasma treatment was applied to both surfaces for 1 min to enable bonding between the two PDMS layers. Figure 3 shows a photograph of the prototype microfluidic system.

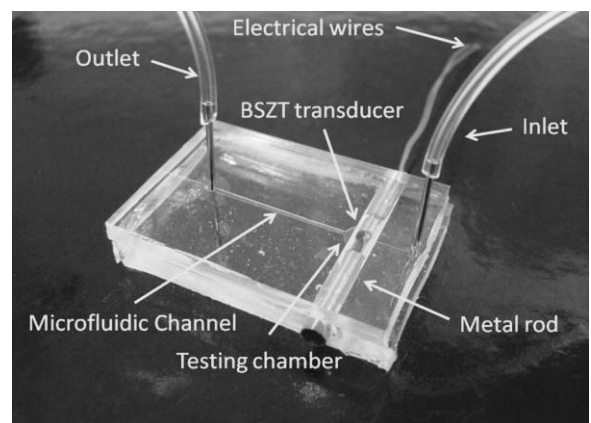


FIG. 3. (Color online) A photograph of the microfluidic system.

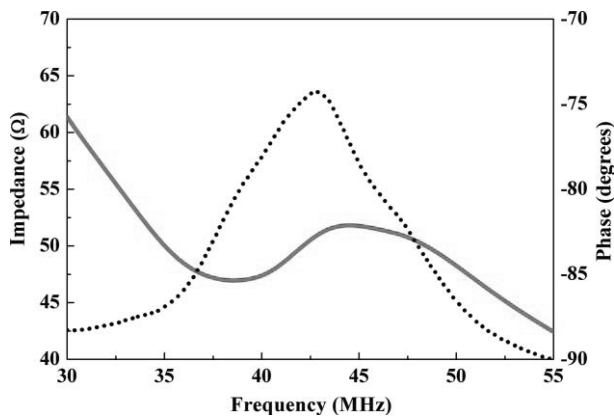


FIG. 4. (Color online) Electrical impedance magnitude and phase angle of the BSZT transducer.

III. RESULTS AND DISCUSSION

The electrical impedance versus frequency of the transducer was measured by an HP4194A impedance analyzer (Fig. 4). The electrical impedance is $\sim 50 \Omega$ near the maximum of the phase angle (~ 43 MHz). From the measured pulse-echo waveform as shown in Fig. 5, the center frequency is found to be ~ 43 MHz and the -6 dB bandwidth is 56.1%. The two-way insertion loss was found to be -26 dB at the center frequency, which is higher than that of the PMN-PT transducer⁶ (-15.8 dB) presumably due to the higher $\tan \delta$ ($= 2.5\%$) of BSZT (in PMN-PT, $\tan \delta = 0.5\%$).

In this system, the transducer acts as both transmitter and receiver. An electrical signal is delivered to the transducer by a function generator to produce a pulse; the pulse is reflected by the metal surface and received by the same transducer after a time delay. Sound velocity c could be calculated by

$$c = \frac{2d}{t}, \quad (3)$$

where d is the distance between the transducer and the reflector and t is the time of flight.

Sodium chloride (NaCl) and potassium chloride (KCl) solution with different concentrations are used as testing

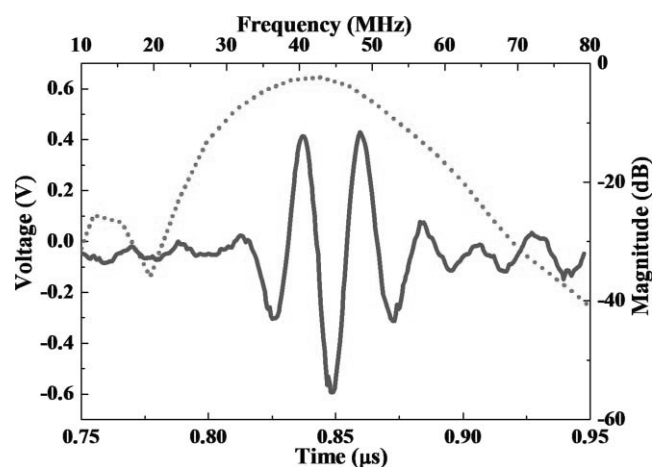


FIG. 5. (Color online) Measured pulse-echo waveform and frequency spectrum of the BSZT transducer.

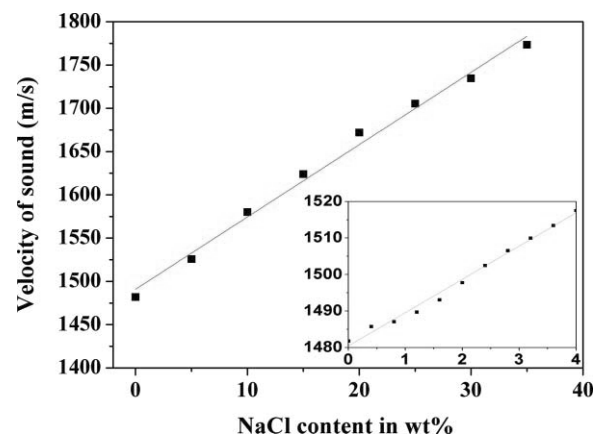


FIG. 6. (Color online) Sound velocity of water–NaCl solution with wt. % from 0% to 35%. Inset: Sound velocity of water–NaCl solution with wt. % from 0% to 4%.

samples. Each solution was pumped using a syringe pump (Baoding Longer Precision Pump Co., Ltd., model TS2–60) and flew through the microchannel at a rate of $20 \mu\text{l/h}$. The measured sound velocity of water at 22°C is 1481.8 m/s, which is close to the reported value.¹² The sound velocity of the saline solution with different weight percentages of NaCl was measured and the results are shown in Fig. 6. It can be seen that the lead-free transducer is capable of sensing the effect of low concentration as shown in Fig. 6(a). Figure 6(b) shows that the velocity of sound increases linearly as the concentration of NaCl increases. Figure 7 shows similar phenomenon with KCl solution. The results obtained from low concentration tests depend on the resolution of the measuring instrument. The slopes of acoustic velocity versus wt. % of KCl and NaCl are found to be 4.5 and $8.5 \text{ ms}^{-1} \text{ wt. \%}^{-1}$, respectively. These results are in agreement with the reported values.¹³ Besides, the acoustic velocity and attenuation coefficient of alcohol ($\text{C}_2\text{H}_5\text{OH}$) were also measured. The attenuation coefficient α is determined by

$$\alpha(f) = \frac{20}{2d} \left(\log_{10} \frac{A_1(f)}{A_2(f)} \right), \quad (4)$$

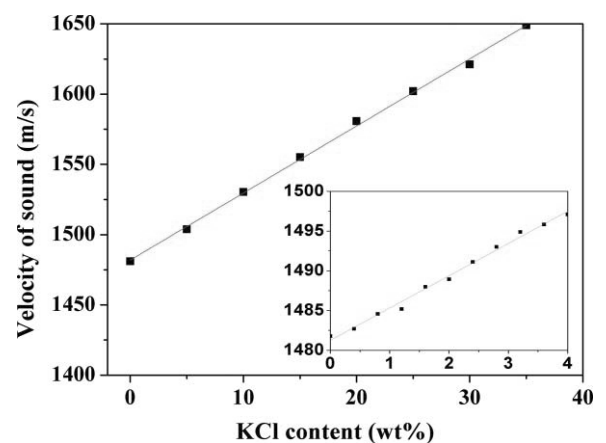


FIG. 7. (Color online) Sound velocity of water–KCl solution with wt. % from 0% to 35%. Inset: Sound velocity of water–KCl solution with wt. % from 0% to 4%.

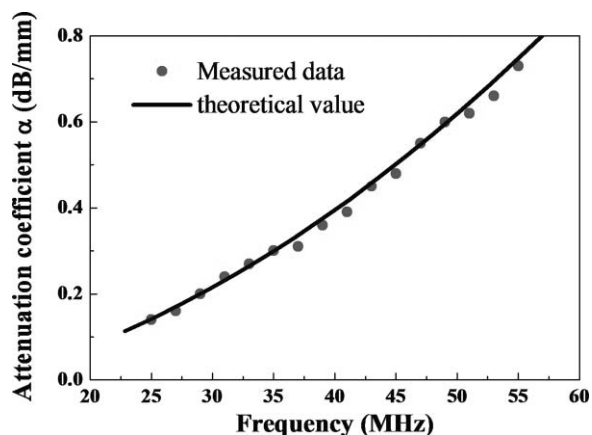


FIG. 8. (Color online) Attenuation coefficient of alcohol at different frequencies. Solid line: obtained from literature values.

where $A_1(f)$ and $A_2(f)$ are the peak-to-peak voltage measured in water and alcohol, respectively.

The sound velocity of alcohol is determined to be 1160 m/s, and Fig. 8 shows the variation of attenuation coefficients of alcohol at different frequencies. The attenuation was found to increase with the frequency and these results agree with literature.^{14,15} Compared with the lead-based materials,⁶ the results suggest that the sensitivity of the lead-free transducer can be comparable. It can be concluded that the use of the lead-free transducer for the application of acoustic properties measurement can provide high sensitivity, high resolution, and the ability to cover a large range of concentrations.

IV. CONCLUSION

We have reported the design and fabrication of a high-frequency ultrasound transducer made from the lead-free

BSZT ceramic. By integrating the transducer into a microchannel, a fast and accurate measurement could be made with a small amount of liquid. This suggests the potential of using this device for biomedical and industrial applications. For example, the rheological properties of blood or petrol, such as velocity and attenuation, can be evaluated by this system.

ACKNOWLEDGMENTS

This work was supported by PolyU internal account 1-ZV5K. Thanks are also due to Dr. S. H. Choy and Mr. N. Y. Chan for their technical support.

- ¹D. J. Harrison, K. Fluri, K. Seiler, Z. Fan, C. S. Effenhauser, and A. Manz, *Science* **261**, 895 (1993).
- ²F. Vinet, P. Chaton, and Y. Fouillet, *Microelectron. Eng.* **61**, 41 (2002).
- ³P. Darlo, M. C. Carrozza, A. Benvenuto, and A. Menciassi, *J. Micromech. Microeng.* **10**, 235 (2000).
- ⁴T. P. Burg, M. Godin, S. M. Knudsen, W. J. Shen, G. Carlson, J. S. Foster, K. Babcock, and S. R. Manalis, *Nature (London)* **446**, 1066 (2007).
- ⁵A. Manz and J. C. T. Eijkel, *Pure Appl. Chem.* **73**, 1555 (2001).
- ⁶S. T. Lau, L. B. Zhao, H. L. W. Chan, and H. S. Luo, *Sens. Actuators A* **161**, 78 (2010).
- ⁷K. K. Shung, and M. Zipparo, *IEEE Trans. Eng. Med. Biol.* **15**, 20 (1996).
- ⁸Y. Saito, H. Takao, T. Tani, T. Nonoyama, K. Takatori, T. Homma, T. Nagaya, and M. Nakamura, *Nature (London)* **432**, 84 (2004).
- ⁹M. D. Maeder, D. Damjanovic, and N. Setter, *J. Electroceramics* **13**, 385 (2004).
- ¹⁰X. G. Tang, X. X. Wang, K. H. Chew, and H. L. W. Chan, *Solid State Commun.* **136**(2), 89 (2005).
- ¹¹W. C. Xu, K. H. Lam, S. H. Choy, and H. L. W. Chan, *Integr. Ferroelectr.* **89**, 87 (2007).
- ¹²J. Lubbers and R. Graaff, *Ultrasound Med. Biol.* **24**, 1065 (1998).
- ¹³R. Barthel, *J. Acoust. Soc. Am.* **26**, 227 (1953).
- ¹⁴L. E. Kinsler, A. R. Frey, A. B. Coppens, and J. V. Sanders, *Fundamentals of Acoustics*, 4th ed. (Wiley, New York, 2002).
- ¹⁵See http://www.ondacorp.com/tecref_acoustictable.shtml for Acoustic Properties of Liquids (Onda Corporation, 2003).